IEEE Access
Multidisciplinary | Rapid Review | Open Access Journal

Received 25 August 2022, accepted 14 September 2022, date of publication 19 September 2022,
date of current version 27 September 2022.

Digital Object Identifier 10.1109/ACCESS.2022.3207762

RESEARCH ARTICLE

First Flight-Testing of LoRa Modulation in Satellite Radio Communications in Low-Earth Orbit

ALEXANDER M. ZADOROZHNY[1], ALEXANDER A. DOROSHKIN[1], VASILY N. GOREV[1], ALEXANDER V. MELKOV[2], ANTON A. MITROKHIN[1,2], VITALIY YU. PROKOPYEV[1], AND YURI M. PROKOPYEV[1]

[1]Division for Aerospace Research, Novosibirsk State University, 630090 Novosibirsk, Russia
[2]OKB Fifth Generation Ltd., 630090 Novosibirsk, Russia

Corresponding author: Alexander M. Zadorozhny (zadorozh@phys.nsu.ru)

ABSTRACT At present, the use of LoRa modulation in satellite radio communications and the construction of a CubeSat constellation for the satellite Internet of Things based on LoRa technology has already begun. However, the limits of applicability of LoRa modulation in low-Earth orbits have not yet been established. This paper presents the results of the first flight tests of LoRa modulation for robustness against the Doppler effect in the satellite-to-Earth radio channel, carried out using a NORBY CubeSat operating at 560 km. Flight tests confirmed the very high immunity of LoRa modulation to the Doppler effect for modes with spreading factor $SF \leq 11$ and spread spectrum modulation bandwidth $BW > 31.25$ kHz. LoRa modulation in these modes can be used in satellite communication without any limitations caused by the Doppler effect. For $BW = 31.25$ kHz, the LoRa radio channel is affected by the static Doppler effect. Communication with the satellite is possible in this case only at high elevation angles. For $SF = 12$, the dynamic Doppler effect becomes significant, and communication is possible only at low satellite elevation angles, which leads to the formation of a ''hole'' in the center of the coverage area directly below the satellite. In both cases, the duration of the communication session is significantly reduced because of the Doppler effect. In the case of $SF = 11$ and 12 at $BW = 31.25$ kHz, both static and dynamic Doppler effect catastrophically affect the LoRa radio channel, so that communication with the satellite becomes impossible.

INDEX TERMS CubeSat, Doppler effect, the Internet of Things, LoRa modulation, low-Earth orbit, on-orbit flight test, satellite IoT, satellite radio communication.

I. INTRODUCTION

The patented LoRa modulation scheme [1] is widely used in existing wireless Internet of Things (IoT) networks [2], [3]. This type of modulation is based on the chirp spread spectrum (CSS) technique, where data are encoded by a wideband chirped signal in which the frequency increases or decreases linearly with time [4], [5]. The main advantages of the CSS technique are lower transmission power requirements and inherent robustness against channel degradation mechanisms, such as multipath, fading, and Doppler effects. LoRa modulation improves the receiver sensitivity by up to 20 dB compared with conventional frequency shift keying (FSK). This enables either a longer range (LoRa) of communication or a reduction in transmit power, thereby reducing the power consumption of the transmitter [4].

The long range of communication provided by LoRa modulation and its resistance to the Doppler effect are important properties not only for terrestrial IoT technologies. LoRa is currently considered as one of the most promising technologies for use in satellite IoT projects based on constellations of satellites in low Earth orbits (LEO) [6], [7], [8], [9]. In particular, the possibility of using constellations of very small satellites of the CubeSat class to create satellite IoT networks

The associate editor coordinating the review of this manuscript and approving it for publication was Sathish Kumar.

has been considered [10], [11]. The low transmission power provided by LoRa modulation makes it extremely attractive for use in conventional CubeSat radio systems.

The very high and time-varying relative velocity between a satellite in Earth orbit and a ground station requires very high robustness of the satellite-to-ground radio channel against the Doppler effect. However, the LoRa modulation specification does not contain clear criteria for its applicability under extreme conditions where the Doppler frequency shift changes rapidly with time.

In [12] and [13], the robustness of LoRa modulation against the Doppler effect in a satellite radio channel was studied experimentally in a laboratory. An LoRa transceiver based on the SX1278 chip from Semtech [14] was used in the experiments. The experiments confirmed the high immunity of LoRa modulation to the Doppler effect for the modulation modes studied. According to [12], this immunity allows for the use of LoRa modulation in satellite radio communications in orbits above 550 km without any restrictions associated with the Doppler effect at any spreading factor SF and spread spectrum modulation bandwidth $BW \geq 125$ kHz. However, experiments have shown that in lower orbits, the time-varying Doppler shift (dynamic Doppler effect) can lead to destruction of the satellite-to-ground radio channel when using the LoRa modulation mode with a maximum spreading factor of $SF = 12$. LoRa modulation modes with $BW < 125$ kHz, which are more sensitive to the Doppler effect, have not been tested in [12] and [13].

The impact of the Doppler shift and Doppler rate on the LoRa satellite-to-Earth radio channel was also analyzed in [15] and [16]. In [16], laboratory studies similar to ours [13] were conducted using the LoRa transceiver SX1261 [17]. The impact of ionospheric scintillation on LoRa satellite radio communication has been studied [18]. Various enhancements to LoRa technology have been proposed to increase the efficiency of the satellite IoT [19], [20], [21]. Moreover, several CubeSats with LoRa devices onboard have already been launched into low-Earth orbits. Thus, in [22], a communication test on CubeSat TRICOM-1R was reported. The LoRa signal was successfully received aboard TRICOM-1R from a ground-based transmitter with a power of only 8 mW. For more than a year and a half, a radio channel based on LoRa modulation has been successfully operating at the NORBY CubeSat [23]. It is used to transmit telemetry information from the satellite and receive control commands from the Earth. In addition, the software is loaded into the NORBY subsystems during debugging also via the LoRa radio channel. Lacuna Space has begun to build a CubeSat constellation for its satellite IoT network. Collaboration between Lacuna Space and Semtech Corporation is expected to begin commercial satellite IoT services based on LoRa technology in the first half of 2022 [24].

However, despite the studies carried out and the started application of LoRa satellite communication, the limits of its applicability in low Earth orbits, determined by the Doppler effect, have not yet been established. Detailed studies of LoRa modulation directly in the satellite-to-Earth radio channel have not yet been carried out.

TABLE 1. NORBY basic subsystems.

Subsystem	Description
Structure	6-Unit CubeSat structure
Electrical Power System (EPS)	Solar panels and battery packs
On-Board Radio Complex (BRC)	UHF transceiver. Control functions
Attitude Determination and Control System (ADCS)	DSG sensor module: – Sun/Earth sensors – 3-axis magnetic sensor – 3-axis angular velocity sensor – 3-axis accelerometer – Temperature sensor A magnetic control system GLONASS receiver
Payload	Registration of gamma rays and charged particles Testing of SpaceFibre/SpaceWire technology

In this paper, we present the results of the first flight tests of LoRa modulation for robustness against the Doppler effect in a satellite-to-Earth radio channel. Onboard experiments were carried out using the NORBY CubeSat operating in a low-Earth orbit [23]. The main purpose of the onboard experiments was to verify the results of our laboratory studies of LoRa modulation [13] and to determine the limits of applicability of LoRa modulation in satellite radio communications in low Earth orbits. Particular attention in the conducted experiments was given to LoRa modulation modes with $BW < 125$ kHz, which have not been tested in the laboratory. An important goal of the experiments was to detect, under real conditions, the effect of radio communication disruption predicted in [13] owing to the dynamic Doppler effect when the satellite passes directly over the ground station.

The remainder of this paper is organized as follows. Section 2 describes the methodology of on-orbit experiments. The results of the experiments are presented in Section 3. A summary of the results and conclusions are provided in Section 4.

II. METHODOLOGY OF ON-ORBIT EXPERIMENTS

A. NORBY CubeSat

Nanosatellite NORBY is a 6U CubeSat designed for flight tests of a new CubeSat-compatible platform developed by Novosibirsk State University [23]. NORBY also carries a payload for the registration of gamma rays and charged particles as well as for testing SpaceFibre/SpaceWire technology. The LoRa transmitter, which is part of the onboard radio system, is essentially a payload for on-orbit studies of LoRa modulation in satellite radio communication.

The NORBY CubeSat was successfully launched on 28 September 2020 by a Soyuz-2.1b carrier rocket from the Plesetsk cosmodrome into a near-polar orbit with an inclination of 97.7 °, apogee of approximately 579 km, and perigee of 545 km.

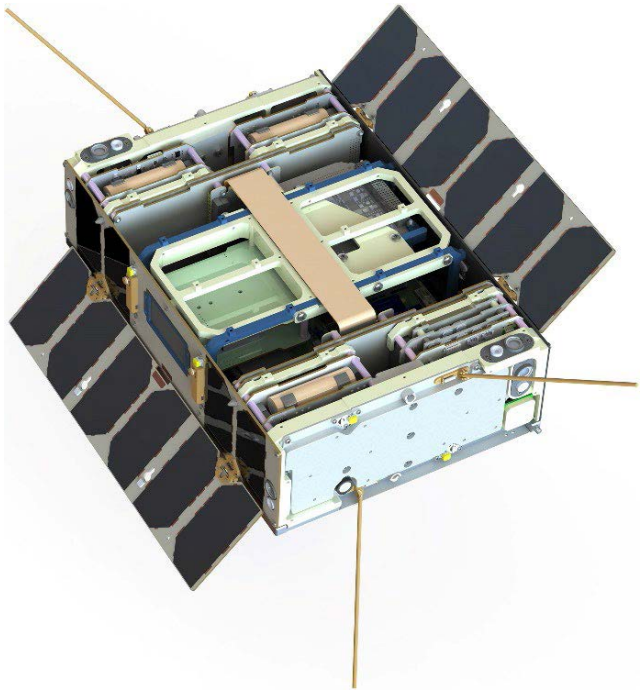

FIGURE 1. General view of NORBY without external cover with solar panels on the large side of the satellite.

A distinctive feature of NORBY is the complete hardware redundancy of all subsystems and information interfaces, which is embedded in the nanosatellite design to improve its reliability. A list of subsystems used in NORBY is presented in Table 1. An external view of the NORBY is shown in Fig. 1. A detailed description of NORBY subsystems can be found in [23] and [25]. Here, we note only those features that are important for the LoRa modulation experiments.

The NORBY on-board radio complex (BRC) uses a Semtech SX1278 transceiver [14]. In addition to the traditional FSK, GFSK, MSK, and GMSK modulation methods, the SX1278 transceiver supports LoRa modulation.

During the development of the BRC, we conducted laboratory and outdoor experimental studies to determine the possibility of applying LoRa modulation in CubeSat radio communication systems [12], [13]. The experiments showed that LoRa modulation has very high immunity to the Doppler effect. Therefore, LoRa modulation was chosen as the main modulation type in BRC for radio communication between the NORBY and the ground control station.

For more than a year, telemetry and data from NORBY payloads have been successfully delivered to the ground station via the LoRa radio channel, and control commands have been transmitted from the ground station to NORBY. The LoRa radio channel is also used to upload software to NORBY for in-orbit software updates, which are required when debugging on-board subsystems.

In accordance with the adopted concept of complete hardware redundancy of subsystems, NORBY has two identical onboard radio systems. Only one of them can operate at any given time. If the active BRC fails, it is switched off, and the second BRC is switched on. Active BRC can also be selected by commands from the ground station.

The NORBY on-board radio complex operates in the UHF band at a frequency of 436.7 MHz. It should be noted that NORBY CubeSat was not created to demonstrate any technologies for satellite IoT, and its on-board radio complex was originally intended to transmit telemetry and data from payloads to the ground control complex. Therefore, the frequency range most frequently used on CubeSats was chosen for BRC. Already in the process of implementing the project, the idea arose to test LoRa modulation for resistance to the Doppler effect, including with LoRa modulation parameters that are interesting for IoT. And we used a tool that was already ready for this – BRC, although it does not work in the traditional IoT frequency range. We also note that the NORBY-2 project currently being implemented is initially focused on demonstrating and testing the capabilities of LoRa modulation in satellite IoT in the 868 MHz and 2.4 GHz frequency bands.

The output power of the BRC transmitter is adjustable in the range of 0.1 to 4 W. At present, the default LoRa modulation parameters for NORBY radio sessions with the ground station are $SF = 10$ and $BW = 250$ kHz, with an emitted BRC transmitter power of 0.2 W. When NORBY is out of range with the ground station, it transmits a beacon signal once per minute containing basic telemetry data regarding the state of NORBY. The beacon is transmitted alternately in the LoRa and GFSK modes at a transmitter output power of 0.2 W. Thus, the LoRa beacon is transmitted only once every two minutes.

The antenna of each BRC is a pair of quarter-wave vibrators located at one of the ends of the satellite body (Fig. 1). The antennas located at different ends of the satellite body are completely identical. During the experiment, only one BRC with its own antenna worked. The second was in reserve. The radiation pattern of the NORBY antenna calculated using the RF Module of COMSOL Multiphysics Simulation Software is shown in Fig. 2. Here, the Z-axis is directed perpendicular to the end face of the satellite body, while the X- and Y-axes are directed perpendicular to the large and small sides of the body, respectively. The radiation pattern was calculated for the antenna with the satellite body including the deployed solar panels. Figure 2 shows that the calculated nonuniformity of the radiation pattern of the NORBY antenna is approximately 7 dB.

At the time of LoRa modulation testing, the NORBY attitude determination and control system was in the debugging stage. All orientation sensors were tested and operational. The magnetic control system was able to slow down the rotation of the satellite to approximately 0.1 °/s and spin it, if necessary, relative to any axis.

B. GROUND STATION FOR RADIO COMMUNICATION WITH A SATELLITE

Similar to the NORBY on-board radio complex, our ground station uses a Semtech transceiver [14] to communicate with

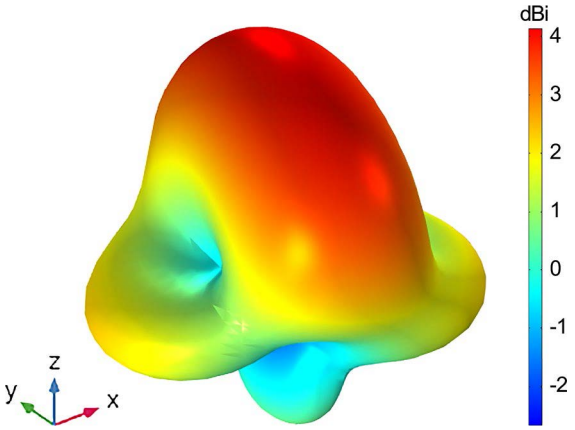

FIGURE 2. Calculated radiation patterns of the NORBY antenna.

FIGURE 3. Ground station antenna.

the satellite. The ground station's steerable antenna system consists of two crossed Yagi-Uda antennas (Fig. 3). The antenna system is installed on the roof of the university's physics department building on a 4-metre high mast. The calculated width of the main beam of a single Yagi-Uda antenna is approximately 30°. The antenna gain is 14.5 dBi.

The antenna is driven by a BIG-RAS/HR azimuth and elevation rotator [26]. The Gpredict program [27] is used to point the antenna at the satellite, which allows the real-time tracking of satellites and prediction of the orbit. Gpredict calculates antenna pointing angles based on a two-line element set (TLE) from the SATCAT catalogue [28]. The NORBY satellite catalog number is 46494.

The rotator provides continuous pointing of the antenna to the LEO satellite over the entire range of visibility of the satellite from the ground station. However, when the satellite passes a region close to the zenith, the antenna cannot accurately track the satellite due to the known keyhole problem [29], which is inherent in antennas with an azimuth and elevation type tracking mount. To clarify the problem, consider the behavior of the antenna when tracking a satellite flying near the zenith in a circular polar orbit (see Fig. 4). In Figure 4, H is the orbit height, v is the satellite velocity, α is the satellite azimuth, and θ is the satellite elevation angle. If we do not take into account the sphericity of the Earth, then by simple mathematical transformations it is easy to obtain an expression for the azimuth angular velocity of the satellite relative to the antenna ω_a:

$$\omega_a = \frac{v \cdot \sin^2 \alpha}{H} \tan \theta_{\max} \tag{1}$$

where $\theta_{\max}$ is the maximum elevation angle of the satellite at the point of the trajectory closest to the antenna at $\alpha = 90°$. It can be seen from (1) that as $\theta_{\max}$ approaches 90°, ω_a increases without limit. That is, the antenna, when accurately tracking the satellite near the zenith, must rotate very quickly around the vertical axis. When the satellite approaches the zenith along a trajectory with $\theta_{\max} = 90°$, the antenna in our case is constantly oriented to the south in the horizontal plane, and at the moment the satellite passes the zenith, it should instantly reorient to the north. Naturally, no real antenna can do this, since it takes some time.

The bottom panel of Fig. 4 shows ω_a in the entire satellite visibility zone calculated using a more accurate numerical model that takes into account the sphericity of the Earth. The calculations were performed for several NORBY trajectories with different $\theta_{\max}$. Here and below, it is assumed that the satellite passes the trajectory point closest to the antenna at time $t = 0$. The red dotted line in Fig. 4 shows the maximum angular velocity of the antenna rotation provided by the azimuth rotator. It can be seen from Fig. 4 that near the zenith, when tracking a satellite on trajectories with $\theta_{\max}$ greater than about 70°, the azimuth angular velocity of the antenna required for accurate tracking exceeds the angular velocity provided by the antenna rotator. As a result, the antenna lags behind the direction to the satellite. The lag of our antenna can be up to about 37° causing the satellite leaves the main beam of the antenna. The result is attenuation of the received radio signal, which becomes noticeable at satellite elevation angles greater than 80° and can reach about 20 dB at angles greater than about 85°.

The considered effect manifests itself at large satellite elevation angles near the zenith. However, it is precisely when the satellite moves in this area that the maximum values of the Doppler rate are reached [13]. That is, possible failures of the LoRa radio channel due to the dynamic Doppler effect are expected primarily in this section of the satellite trajectory.

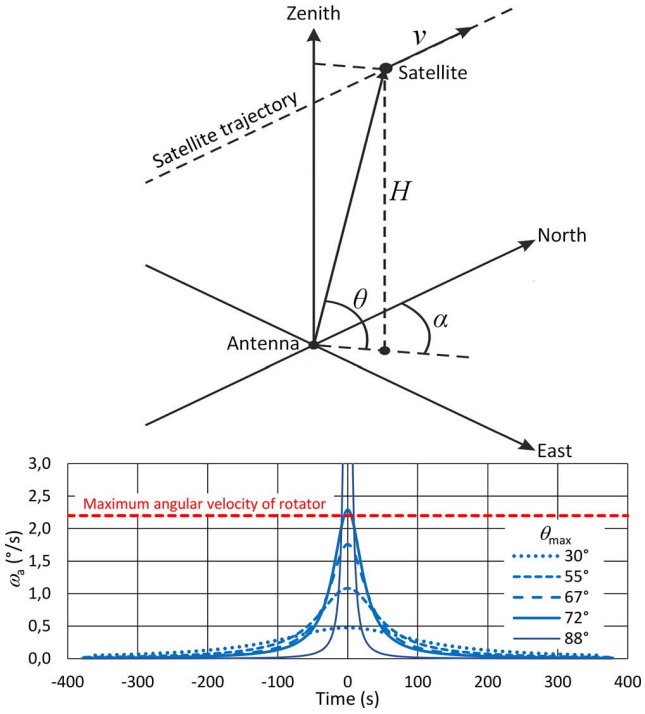

FIGURE 4. Flight pattern of the satellite over the ground station antenna and the angular velocities of the azimuth rotator required to track the satellite on trajectories with various maximum elevation angles θ_{max}. The red dashed line is the maximum possible angular velocity of the antenna rotator. The moment of time $t = 0$ is taken to be the moment when the satellite passes the point of the trajectory closest to the ground station.

In this case, in order to unambiguously identify the impact of the dynamic Doppler effect, any other possible causes of the radio communication failure should be excluded. Therefore, to exclude possible radio communication disruptions due to inaccurate antenna pointing, we conducted our experiments at the maximum emitted power of the NORBY transmitter.

C. CONDUCTING THE EXPERIMENT

The testing of LoRa modulation in satellite-to-ground radio communication is organized as follows. After receiving a beacon signal from NORBY, when it enters the radio visibility zone, the ground station operator sends a command to the satellite to turn on the transmission mode of the sequence of data packets. The command contains information about the required LoRa modulation parameters, packet size L, number of transmitted packets N and transmitter power (4 W). A timing diagram for the transmission of data packets during the experiment is shown in Fig. 5. After receiving the command, the NORBY on-board radio system switches to mode with the specified LoRa modulation parameters and transmitter power. Subsequently, the transmission of N data packets of a given size begins. Each data package contains the following:

- the sequence number of the packet in the sequence;
- current navigation data from the GLONASS receiver (time, coordinates, and speed of the satellite);
- brief telemetry information.

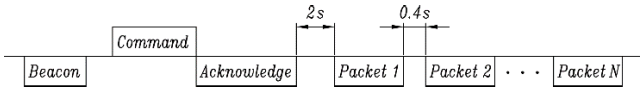

FIGURE 5. Timing diagram of the transmission of data packets from the NORBY satellite during the experiments.

Upon completion of the transmission of the N-th packet, BRC returns to the original mode of transmitting beacon signals with a power of 0.2 W.

It should be noted that because NORBY transmits the LoRa beacon at two-minute intervals, packet transmission begins with an unpredictable delay of up to two minutes after the satellite enters the radio coverage area of the ground station. In cases in which the ground station operator did not manage to send a command in time, this delay is even greater.

The main purpose of the experiments was to identify the influence of the Doppler effect on the stability of the satellite LoRa radio channels. Therefore, during the experiments, LoRa packets were transmitted at the maximum possible power of the BRC transmitter of 4 W to avoid possible radio communication disruptions owing to a weak signal or external noise.

The SX1278 transceiver includes a received signal strength indicator (RSSI), signal-to-noise ratio (SNR) meter, and an indicator of the frequency difference between the carrier frequency of the signal at the receiver input and the carrier frequency of the receiver (frequency error, FER) [14]. All of these parameters are recorded when a LoRa packet transmitted from NORBY is received at a ground station.

Thus, as a result of each experiment during the NORBY flyby over the ground station, we obtained the following information:

- the number of packets transmitted from the satellite;
- number of lost packets;
- packet transmission times, including lost ones;
- the location and speed of the satellite at the time of each packet transmission;
- RSSI, SNR and FER for each received packet.

The data obtained allows us to determine the Doppler frequency shift in the satellite radio channel for each data packet. The Doppler shift can be directly calculated from satellite trajectory data. During the experiment, trajectory data were received from the GLONASS receiver onboard NORBY. In addition, they can be determined from TLE data from the SATCAT catalog [28]. If the transmitter emits a radio signal with frequency F_0, owing to the Doppler effect, the receiver receives a signal with frequency [13]

$$F = \frac{1}{1 + \frac{v}{c}\cos\beta} \cdot F_0 \tag{2}$$

where v is the satellite velocity, n is the light speed, β is the angle between the satellite velocity vector and the direction to the ground station. Then, the Doppler frequency shift ΔF_D can be expressed as

$$\Delta F_D = F - F_0 = [1/(1 + \frac{v}{c} \cdot \cos\beta) - 1] \cdot F_0. \tag{3}$$

Note that the TLE data can be used to determine the Doppler shift for both the received and lost packets.

An additional contribution to the total frequency offset ΔF between the input signal and carrier frequency of the LoRa receiver also comes from the frequency difference between the reference oscillators of the receiver and transmitter ΔF_{RT}:

$$\Delta F = \Delta F_D + \Delta F_{RT}. \tag{4}$$

We don't know of any other reasons that could contribute to ΔF.

Fig. 6 shows the ΔF_D and ΔF obtained from a NORBY flyby over a ground station. The Doppler shift was derived from both the GLONASS and TLE-based trajectory data. The total frequency offset was obtained from the FER data of the ground station LoRa receiver. Here and below, the moment of time $t = 0$ is taken as the moment when the satellite passes the point of the trajectory closest to the ground station. It can be seen that the results of determining the Doppler shift from the TLE data and the data of the GLONASS receiver practically coincide. The total frequency offset differs somewhat. According to (4), we assume that this difference is due to ΔF_{RT}. This assumption is also confirmed by the observed change in $\Delta F - \Delta F_D$ over time.

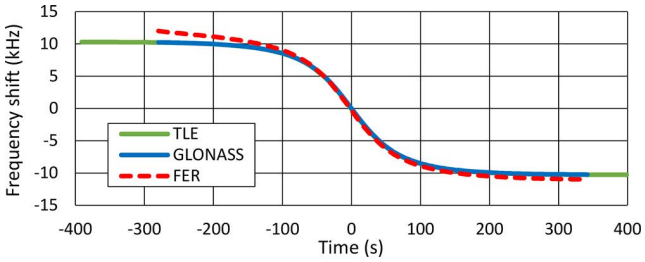

FIGURE 6. Comparison of the Doppler shift according to the TLE and GLONASS data with the total frequency shift according to the FER data obtained during the NORBY flight over the ground station. The moment of time $t = 0$ is taken to be the moment when the satellite passes the point of the trajectory closest to the ground station.

A maximum $\Delta F - \Delta F_D$ value of approximately 1.8 kHz was observed at the beginning of the radio session. By the end of the experiment, it had dropped by about 2.5 kHz to -0.7 kHz. This decrease in $\Delta F - \Delta F_D$ is naturally explained by the change in the carrier frequency of the NORBY transmitter, caused by the heating of the reference crystal oscillator. The crystal oscillator is located on the BRC PCB close to the transmitter power amplifier, which dissipates approximately 4 W of thermal power. The temperature dependence of the frequency of the transmitter reference oscillator was studied during pre-flight ground tests of the BRC. The crystal oscillator frequency drift in the range from about -20 to $+40$ °C is about -0.2 ppm/°C. This means that the observed decrease in $\Delta F - \Delta F_D$ by 2.5 kHz can be explained by a change in the carrier frequency of the NORBY transmitter due to heating of the reference crystal oscillator by about 30 °C.

This means that the observed 2.5 kHz change in the carrier frequency of the transmitter is caused by heating by approximately 30 °C.

In all experiments performed, the absolute value of $\Delta F - \Delta F_D$ did not exceed 2 kHz. This means that the change in the carrier frequency of the received signal from NORBY is mainly due to the Doppler effect. The frequency difference between the reference oscillators of the receiver and transmitter only makes a small, albeit noticeable, contribution to the total frequency offset.

D. EXPERIMENTAL CONDITIONS

The results of laboratory studies on LoRa modulation have shown that LoRa radio communication with a satellite in low Earth orbit can be disrupted in some cases owing to the dynamic Doppler effect [13]. The maximum absolute value of the Doppler rate is achieved when the satellite passes at the zenith over the ground station (see Fig. 7c). Since possible radio communication disruptions were expected at high Doppler rates, NORBY orbits were chosen for our flight experiments with a maximum satellite elevation above the ground station of more than about 80°.

As noted above, we could not completely stop the rotation of the NORBY CubeSat during the experiments, and orient it in the direction at the ground station. Therefore, during the experiments, NORBY rotated unpredictably, and we ensured that the rotation speed did not exceed a few degrees per second.

As an example, Fig. 7 shows the results of experiment No. 1 with LoRa modulation parameters $SF = 7$ and $BW = 500$ kHz, at which, according to laboratory experiments [13], no influence of the Doppler effect was expected. In total, during the radio communication session in this experiment, 773 packets of size $L = 143$ bytes were transmitted from NORBY, of which 748 packets were successfully received by the ground station and 25 packets were lost.

The green curves in Figures 7a, 7b, and 7c show the elevation angle, Doppler shift ΔF_D, and Doppler rate $\Delta F'_D$, as NORBY passes over the ground station. The elevation angle and Doppler shift were derived from the TLE data. The Doppler rate is determined by differentiating ΔF_D. NORBY was within the radio visibility of the ground station between approximately -370 s and $+370$ s.

The bold blue dots in Figures 7a, 7b, and 7c indicate the elevation angle, Doppler shift, and Doppler rate obtained from the GLONASS receiver data contained in the received packets. Once again, we note that the elevation angle, ΔF_D, and $\Delta F'_D$ obtained based on two different initial data practically coincide. For lost packets, only the TLE data are available. Therefore, in this case, the elevation angle, ΔF_D, and $\Delta F'_D$ were determined from the TLE data and the known time of sending packets from NORBY. The lost packets are marked in Fig. 7 and below with bold red dots.

Figures 7d and 7e show the signal strength (RSSI) and signal-to-noise ratio (SNR) at the input of the ground station receiver for the received packets. There is no such data for the

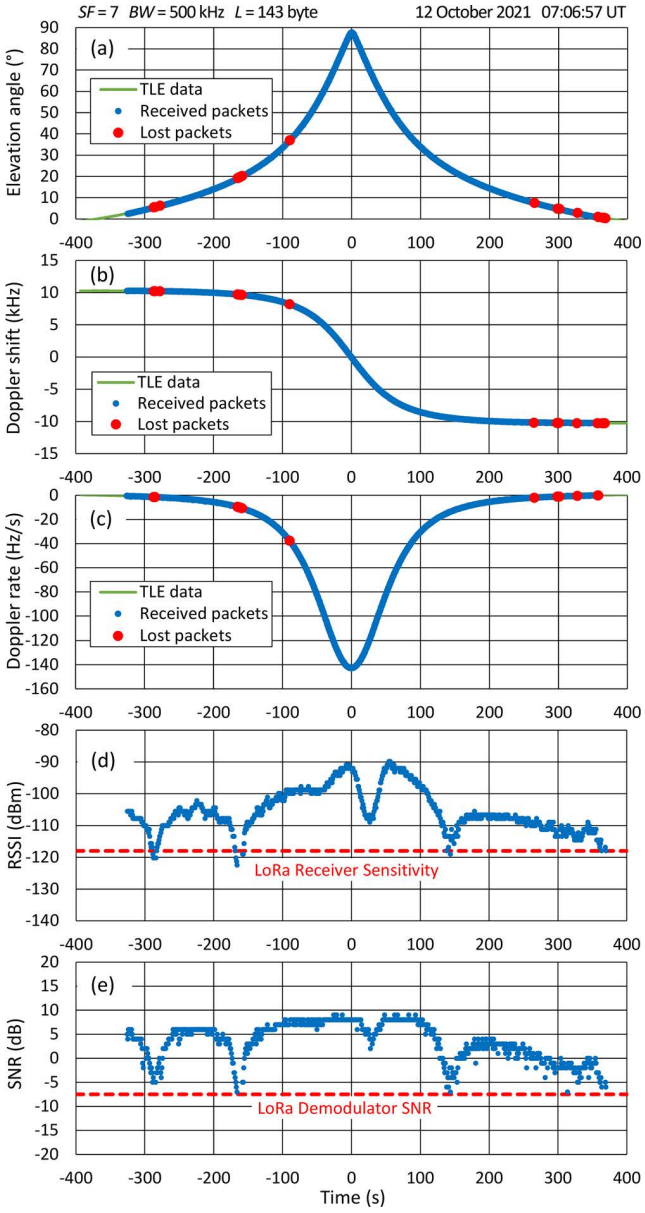

FIGURE 7. Results of experiment No.1 with the LoRa modulation parameters $SF = 7$ and $BW = 500$ kHz: (a) elevation angle, (b) Doppler shift, (c) Doppler rate, (d) signal level RSSI and (e) signal-to-noise ratio SNR at the receiver input. The size of the transmitted packets $L = 143$ bytes. The red dashed lines show the LoRa receiver sensitivity and the minimum allowable SNR value for the SF and BW parameters [14].

lost packets. However, the reasons for their loss can be determined from the behavior of the nearby values of RSSI and SNR. Therefore, it can be seen that packet losses near −280 s and −160 s occurred in the region of a sharp decrease in RSSI and SNR. RSSI has decreased here to the LoRa receiver sensitivity of −118 dBm, and SNR has decreased to the minimum allowable value of −7.5 dB, which corresponds to $SF = 7$ and $BW = 500$ kHz [14]. Such attenuation of the radio signal occurs owing to the non-uniformity of the satellite antenna radiation pattern (Fig. 2) and the rotation of NORBY. It can be noted that Fig. 6d shows that the actual non-uniformity of the radiation pattern of the NORBY antenna noticeably exceeds the calculated 7 dB. The weakening of the signal near the 25th second is due to the delay in pointing the ground antenna near the direction to the zenith. It may also be superimposed by the weakening associated with satellite rotation.

Packet loss at low elevation angles before the satellite leaves the radio visibility zone (Fig. 7d) cannot be explained by a weak signal, which remains above the LoRa receiver sensitivity almost to the horizon. However, in Fig. 7e, in the area of these losses, there are reduced SNR values in the form of points that fall outside of the main data array. Such SNR behavior was observed only in some daytime experiments, during which powerful construction equipment was operating in the immediate vicinity (∼30–50 m) of the ground receiving antenna during the construction of a new university building. We attribute these packet losses to electromagnetic interference generated by this technique.

For a single lost packet at −89 s (Fig. 7), no external causes were found to explain its loss. More than five thousand packets were transmitted from the NORBY CubeSat for all communication sessions during which the described experiments were performed. However, only four such cases were recorded, for which no explanation was found for the loss of the transmitted packet.

As expected, the experiment showed no influence of the Doppler effect on the satellite-to-ground LoRa radio channel with modulation parameters $SF = 7$ and $BW = 500$ kHz.

It should be noted that the RSSI and SNR time variations shown in Fig. 7 also contain variations due to propagation loss. The distance between the satellite and the ground station varies from approximately 560 to 2700 km as NORBY moves in orbit from zenith to horizon. In this case, the signal is attenuated by approximately 13.7 dB. The total variations of RSSI in Fig. 7 are significantly larger than this value. In addition, the transmitter power of 4 W during the experiments ensures the signal value at the LoRa receiver input is significantly higher than the receiver sensitivity, as well as the allowable SNR value right up to the horizon. Therefore, the propagation loss does not affect the results of experiments presented in this section and below.

It should also be noted that we did not check during the experiments for the presence of any other radio transmitters operating in the same frequency range near the ground antenna. However, their presence should show up in the SNR data. Neither in the described experiment No. 1, nor in all the others, no signs of the impact of any third-party radio transmitters were recorded.

Here, we specifically considered the results of the experiment with LoRa modulation parameters $SF = 7$ and $BW = 500$ kHz. The relatively low sensitivity of the LoRa receiver and the relatively low noise immunity in this mode, which was the lowest in the experiments conducted, were the worst for conducting the experiment under non-ideal environmental conditions. The results obtained under these conditions made it possible to illustrate the operability of the equipment used in the experiment and the possibility of an unambiguous interpretation of the data obtained.

E. LoRa MODULATION PARAMETERS

The main objective of this research is to verify under real space conditions the robustness parameters of LoRa modulation to the Doppler effect in the satellite-to-ground radio channel given in the SX1278 transceiver specification [14] and obtained in laboratory experiments [13].

According to [14], the maximum tolerated frequency offset between the transmitter and receiver $\Delta F_{\max}$ is determined by the expression

$$\Delta F_{\max} = 0.25 \cdot BW. \tag{5}$$

For $SF \geq 10$ and $BW \geq 125$ kHz, a tighter limit on $\Delta F_{\max}$ applies [14], but in our case, this is not important. The maximum Doppler shift for the NORBY orbit is approximately 10.2 kHz (see Fig. 6). Consequently, destructive effects of the Doppler shift on satellite-to-ground radio communications can be expected at BW of less than approximately 41 kHz. For this reason, NORBY experiments were carried out not only at $BW \geq 125$ kHz, as in laboratory experiments [13], but also at lower BW values.

The LoRa SX1278 transceiver specification [14] does not provide information about the maximum tolerated rate of change of the frequency offset between the transmitter and receiver $\Delta F'_{\max}$. In laboratory experiments [13], $\Delta F'_{\max}$ was determined for only three pairs of SF and BW values. The minimum value of $\Delta F'_{\max} = 144$ Hz/s was obtained for the pair $SF = 12$ and $BW = 125$ kHz. Such a rate of change in the Doppler shift can only be achieved in orbits below 550 km. This served as the basis for the prediction in [13] of the LoRa radio communication disruption at $SF = 12$ and $BW = 125$ kHz in such low orbits when the satellite passes at the zenith over the ground station. The height of the NORBY orbit is slightly higher, and the Doppler rate reaches only approximately 143 Hz/s in absolute value (Fig. 7c). Therefore, it was not possible to confirm the predicted effect using these LoRa parameters in NORBY experiments. However, its occurrence could be expected for LoRa modulation parameters, which are more sensitive to the Doppler effect at lower BW. In this regard, special attention was paid to the NORBY experiments to test the Lora modulation with $BW < 125$ kHz at SF of 11 and 12.

The list of flight experiments carried out on the NORBY CubeSat and the LoRa modulation parameters used are listed in Table 2. The shaded rows in Table 2 refer to experiments in which the maximum Doppler shift in the NORBY orbit equal to approximately 10.2 kHz (see Fig. 6) is greater than the $\Delta F_{\max}$ value given in the LoRa SX1278 transceiver specification [14] and corresponding to (5). In these experiments, it is expected to register the impact of the static Doppler effect on the LoRa radio channel.

LoRa modulation also includes a variable error correction scheme [14]. In the NORBY experiments, we used a coding rate of 4/5, which ensures the detection of errors in the communication channel, but does not correct them. Packets transmitted from NORBY are considered to be received by the ground station only if they are received without errors. Otherwise, they were considered lost.

It should also be noted that the *LowDataRateOptimize* LoRa modulation parameter was activated during the experiments.

TABLE 2. LoRa modulation parameters used in the NORBY flight experiments.

Exp. No.	SF	BW, kHz	L, byte	LoRa receiver sensitivity, dBm [14]	$\Delta F_{\max}$, kHz [14]	$\Delta F_{\max}$, kHz [13]	$\Delta F'_{\max}$, kHz/s [13]
1	7	500	143	-118	±125		
2	7	125	55	-125	±31.25	±31.0	±65.5
3	7	125	143	-125	±31.25	±31.0	±65.5
4	7	62.5	55	-128	±15.6		
5	7	62.5	143	-128	±15.6		
6[a]	7	31.25	55	-131	±7.8		
7[a]	7	31.25	143	-131	±7.8		
8	10	62.5	55	-135	±15.6		
9	10	62.5	143	-135	±15.6		
10[a]	10	31.25	55	-138	±7.8		
11[a]	10	31.25	143	-138	±7.8		
12	11	62.5	55	-137	±15.6		
13	11	62.5	143	-137	±15.6		
14[a]	11	31.25	55	-140	±7.8		
15[a]	11	31.25	143	-140	±7.8		
16	12	125	55	-137	±21.835	±24.0	±0.14
17	12	125	143	-137	±21.835	±24.0	±0.14
18	12	62.5	55	-140	±15.6		
19	12	62.5	143	-140	±15.6		
20[a]	12	31.25	55	-143	±7.8		

[a]Shaded are experiments in which the Doppler shift in the NORBY orbit was larger than the $\Delta F_{\max}$ given in the LoRa transceiver SX1278 specification [14], i.e., in which radio disruptions due to a large Doppler shift were expected.

III. RESULTS OF EXPERIMENTS

Testing of LoRa modulation in flight experiments on the NORBY CubeSat was carried out for $SF = 7$, 10, 11, and 12 at $BW = 500$, 125, 62.5 and 31.25 kHz and two signal packet sizes $L = 55$ and 143 bytes (Table 2).

Experiments for $SF = 7$ were performed for all selected values of BW. This is a reference series of experiments in which it is expected to register the influence of the static Doppler effect in accordance with the LoRa SX1278 transceiver specification [14]. However, in these experiments, it is not expected to detect any influence on the LoRa radio channel of the dynamic Doppler effect [13]. The main objectives of these experiments are to verify the specifications of the LoRa SX1278 transceiver [14] regarding immunity to Doppler shift and to confirm the robustness of LoRa modulation against the dynamic Doppler effect in NORBY orbit in accordance with laboratory studies [13]. Special experiments with $BW = 250$ kHz were not carried out, since in numerous daily radio sessions of NORBY with the ground station at $SF = 10$ and $BW = 250$ kHz, no influence of Doppler effects on radio communication was ever recorded.

The main objective of experiments with $SF = 10$, 11 and 12 is to detect the influence of the dynamic Doppler effect on LoRa modulation. Laboratory experiments [13] found that LoRa modulation becomes less resistant to Doppler rate as SF increases and BW decreases. Theoretical analysis [18], [19] also shows that as SF increases and BW decreases, the dynamic Doppler effect begins to affect the LoRa radio channel at lower Doppler rates. In this regard, we did not carry out experiments at large BW. For the same reason, we did not conduct experiments with $SF = 8$ and 9.

The results of the experiments grouped by SF are presented in the following sections.

A. SF = 7

Seven experiments were performed using $SF = 7$. The first three experiments, Nos. 1, 2, and 3, were conducted at $BW = 500$ and 125 kHz. The maximum allowable Doppler frequency shift in these modes, according to the specification [14] and laboratory experiments [13], is several times greater than the Doppler shift of approximately 10 kHz owing to the movement of the satellite in low earth orbit (see Table 2). The immunity of LoRa modulation to the Doppler rate at $SF = 7$ and $BW = 125$ kHz, according to [13], is also sufficient with a large margin for using LoRa modulation in satellite radio communications.

Fig. 7, which shows the results of experiment No. 1, fully confirms these conclusions. Despite the presence of a loss of some packets, no influence of the Doppler effect on the LoRa radio channel was found in this experiment. As noted above, the loss of transmitted data packets recorded in this experiment is associated with a weak signal due to the CubeSat orientation and low SNR due to ambient noise. Only for the loss of one packet, no explanation was found.

In experiments No. 2 and No. 3, packets of 55 bytes and 143 bytes, respectively, were transmitted. In experiment No. 2, 597 packets were transmitted, of which 518 were received. In experiment No. 3, 381 packets were transmitted, of which only one was lost. The results of these experiments are similar to those of experiment No. 1. The influence of the Doppler effect, as well as the size of the transmitted packet on the satellite-to-ground LoRa radio channel, was not detected.

It can be noted that in all the experiments carried out, 111 packet losses were recorded, caused by the unsuccessful orientation of the NORBY antenna, interference from construction equipment operating near the ground antenna, and other unexplained reasons. Of these, 104, that is, approximately 94%, are accounted for by experiments No. 1 and No. 2, especially in the second – 79 losses. Analysis of data from the NORBY attitude sensors showed that during experiment No. 2, the CubeSat rotated relatively quickly around the Z-axis and very slowly around the X- and Y-axes. This resulted in a long (approximately 100 s) unsuccessful orientation of the NORBY antenna. A small spin-up of NORBY after this experiment corrected this situation. In experiment No. 8, which was carried out three days later, there were no such losses. In all subsequent experiments, except for experiment No. 1, which was performed last, only one packet loss due to the unsuccessful orientation of the CubeSat antenna was recorded (experiment No. 17). The relatively large number of packet losses due to the unsuccessful orientation of the CubeSat antenna in experiment No. 1 is also due to the low sensitivity of the LoRa receiver at $SF = 7$ and $BW = 500$ kHz, which is significantly less than in other experiments (see Table 2).

Fig. 8 and Fig. 9 show the results of experiments No. 4 and No. 6 with $BW = 62.5$ kHz and 31.25 kHz, respectively. In experiment No. 4, 431 packets were transmitted from NORBY, all of which were successfully received at the ground station. In experiment No. 6, 554 packets were sent, of which only 434 were received.

In experiment No. 4 (Fig. 8), the command to switch to continuous transmission of a sequence of packets was sent to the CubeSat from the ground station only after the arrival of the second NORBY beacon, that is, with an additional two-minute delay. Therefore, the transmission of data packets from NORBY in experiment No. 4 began only at -133 s, approximately four minutes after the satellite entered the radio visibility zone of the ground station. In this experiment, all data packets transmitted from NORBY were successfully received by the ground station. The satellite-to-ground radio channel worked steadily while NORBY was in the radio visibility zone of the ground station, that is, above the horizon. Communication was interrupted only when the satellite's elevation angle became less than about 1.7°.

In experiment No. 6 (Fig. 9), the transmission of packets from NORBY started at t $= -351$ s, but only packet No. 210 was received first at t $= -79$ s when the Doppler shift ΔF_D decreased to 7.7 kHz. Communication with the satellite was again interrupted at $+76$ s, when the Doppler shift again increased in absolute value to 7.6 kHz. Subsequently, the ground station did not receive any data packet. Fig. 9d and Fig. 9e show that in the time interval between -79 s and $+76$ s, both the signal level and signal-to-noise ratio at the receiver input were quite large, significantly exceeding the LoRa receiver sensitivity and LoRa demodulator SNR, respectively. We do not know the values of RSSI and SNR at times when the data packets from the satellite were not received by the ground station. However, the behavior of RSSI and SNR in other experiments (Fig. 7 and Fig. 8) indicates that their abrupt change, leading to the termination of communication with the satellite for a long period, is unlikely. Therefore, we attribute the packet loss observed in experiment No. 6 to the Doppler effect.

As noted above, the total frequency offset ΔF between the carrier frequencies of the input signal and LoRa receiver differs slightly from the Doppler shift because of the difference in the frequencies of the reference generators of the receiver and transmitter (4). Therefore, it is possible to more accurately determine the maximum allowable value of $\Delta F_{\max}$ above which the LoRa radio communication is broken using the FER data of the LoRa receiver of the ground station. In our case, we get $\Delta F_{\max} = 7.8$ kHz and 7.7 kHz for $t = -79$ s

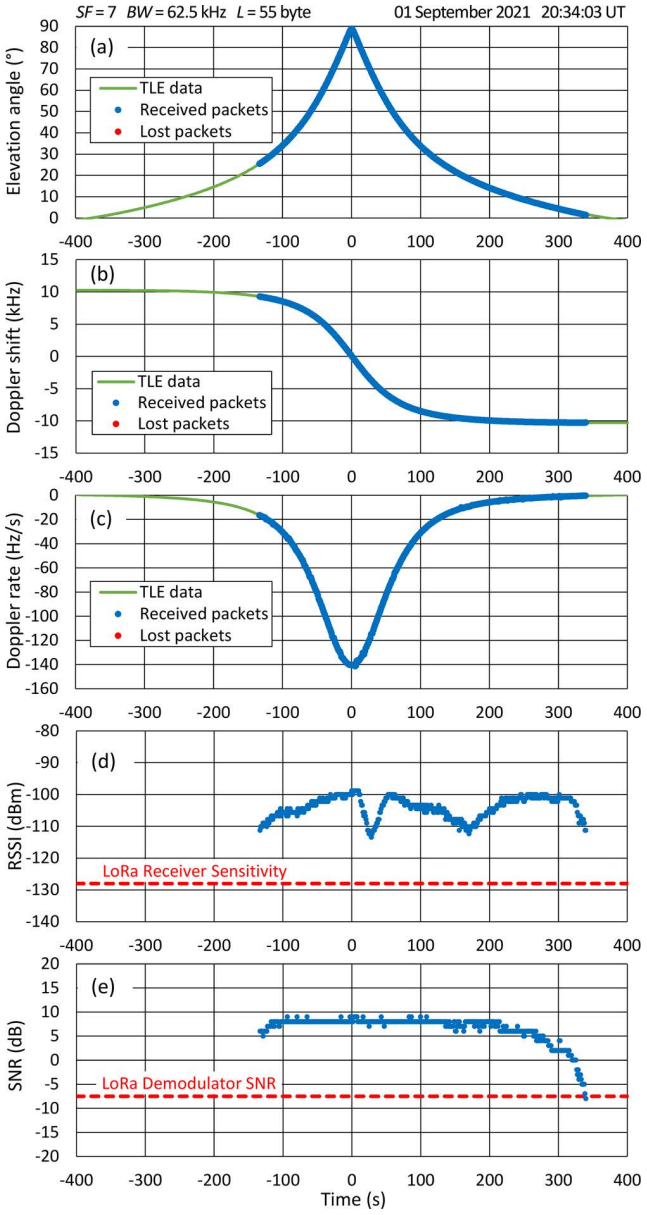

FIGURE 8. Same as Fig. 7 but for experiment No. 4 with the LoRa modulation parameters $SF = 7$, $BW = 62.5$ kHz and $L = 55$ bytes.

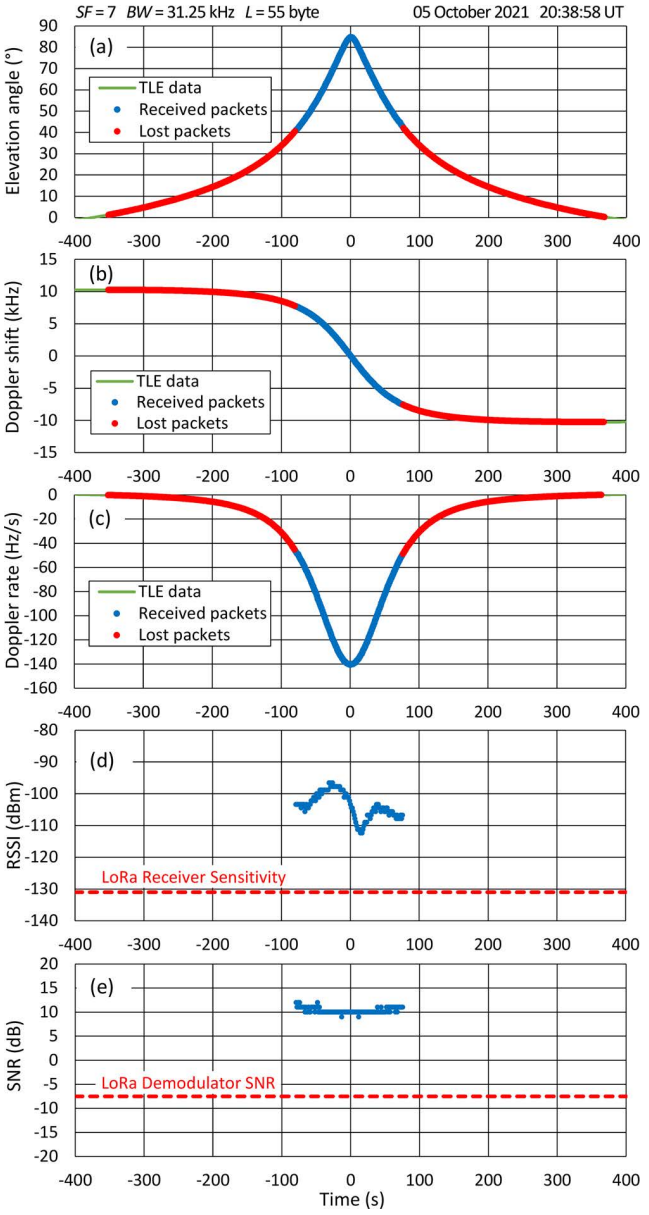

FIGURE 9. Same as Fig. 7 but for experiment No. 6 with the LoRa modulation parameters $SF = 7$, $BW = 31.25$ kHz and $L = 55$ bytes.

and +76 s, respectively. These values agree very well with the maximum tolerated frequency offset between transmitter and receiver $\Delta F_{\max} = 7.8$ kHz for $BW = 31.25$ kHz given in the SX1278 LoRa transceiver specification [14] (see Table 2).

Experiments No. 5 and No. 7 were performed for the same LoRa modulation parameters $SF = 7$ and $BW = 62.5$ and 31.25 kHz as the previous ones, but with longer data packets ($L = 143$ bytes). In experiment No. 5, 493 packets were transmitted, of which only one was lost. In experiment No. 7, out of 348 transmitted packets, 270 were lost. Similar to experiment No. 6, in experiment No. 7, the satellite-to-ground LoRa radio channel worked only at high elevation angles. Packet reception started only when ΔF_D dropped to 8.5 kHz and stopped again at $\Delta F_D = -6.4$ kHz. The conclusion is similar to the previous one: the reason for the destruction of the LoRa satellite-to-ground radio channel in experiment No. 7 is the Doppler shift. According to the FER data, the value $\Delta F_{\max} = 7.7$ kHz was obtained both during a decrease and increase in the absolute value of the Doppler shift.

We did not conduct experiments with $BW = 250$ kHz, since the absence of the influence of the Doppler effect on the LoRa radio channel in experiments with $BW = 500$, 125 and 62.5 kHz gives grounds to assume that it is absent for $BW = 250$ kHz as well. It can also be noted that for almost two years of NORBY operation, we did not find any influence of the Doppler effect in regular radio sessions in the mode $BW = 250$ kHz and $SF = 10$.

B. SF = 10

Four experiments were performed with $SF = 10$ (Table 2). Figures 10 and 11 show the results of two of them, No. 9 and No. 11, performed with packets of size $L = 143$ bytes at $BW = 62.5$ and 31.25 kHz, respectively. In experiment No. 9, NORBY transmitted 230 packets. Three of them were lost. The most likely cause of these losses is electromagnetic interference from construction equipment operating near the ground station during the radio session. As noted above, this is indicated by the reduced SNR values that dropped out of the main dataset in Fig. 10e.

In experiment No. 11, the ground station received only 20 out of the 75 packets transmitted. Note that, with increasing SF and decreasing BW, the time for transmitting one data packet increases. Therefore, the number of data packets transmitted by NORBY per communication session is noticeably reduced in this case.

As expected (see Table 2), experiment No. 11 also demonstrated the destructive effect of the Doppler effect on the satellite-to-ground LoRa radio channel at $BW = 31.25$ kHz. In this experiment, packet transmission started at $t = -199$ s, but only packet No. 19 at $t = -68$ s was received first (see Fig. 11). Communication with the satellite was again interrupted at +78 s, after which the ground station did not receive a single packet. The signal from the satellite appeared when the Doppler shift decreased to 7.1 kHz. Packets began to be lost when the Doppler shift again increased in absolute value to 7.8 kHz. According to the FER data, the values $\Delta F_{\max} = 7.8$ kHz and 7.6 kHz were obtained during decreasing and increasing the absolute value of the Doppler shift, respectively.

Experiments No. 8 and No. 10 were performed for the same LoRa modulation parameters as the previous ones, but with shorter data packets ($L = 55$ bytes). In experiment No. 8, NORBY transmitted 216 packets, all of which were successfully received by the ground station. In experiment No. 10, the satellite-to-ground LoRa radio channel worked again only at high elevation angles. The ground station began receiving data packets from the satellite only when the Doppler shift decreased to 7.7 kHz and then stopped receiving when the ΔF_D again exceeded 7.6 kHz in absolute value. The corresponding values of $\Delta F_{\max}$ are 7.8 kHz and 7.7 kHz.

Thus, the results of experiments with $SF = 10$ fully confirmed the influence of the Doppler effect on the LoRa satellite-to-ground radio channel at $BW = 31.25$ kHz, found in experiments with $SF = 7$.

C. SF = 11

Experiments with $SF = 11$ were also carried out at $BW = 62.5$ and 31.25 kHz (see Table 2). The results of experiments No. 12 and No. 13 at $BW = 62.5$ kHz are similar to the results of experiments with $SF = 7$ and 10, performed at the same spread spectrum modulation bandwidth. In these experiments, 190 and 95 data packets, respectively, were transmitted from NORBY. Only two of them were not received by the ground station in experiment No. 12 for an unidentified reason (see Fig. 12). In these experiments, no influence of the Doppler effect on the satellite-to-ground LoRa radio channel was observed.

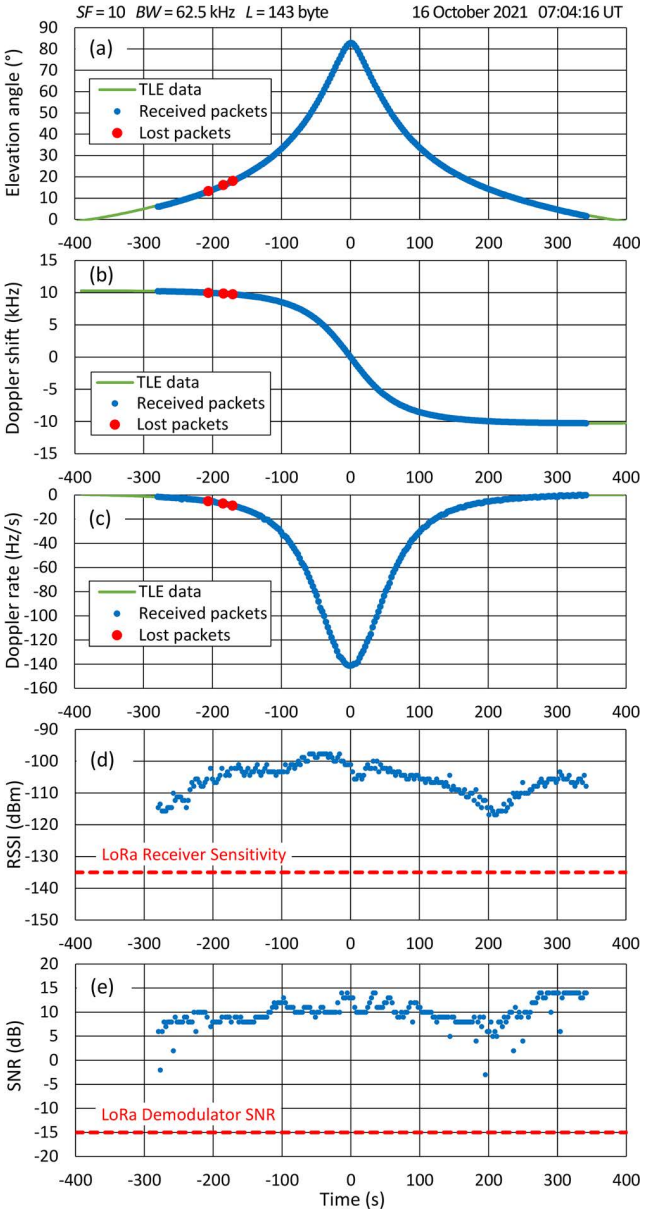

FIGURE 10. Same as Fig. 7 but for experiment No. 9 with the LoRa modulation parameters $SF = 10$, $BW = 62.5$ kHz and $L = 143$ bytes.

The results of experiments No. 14 and No. 15, carried out at $BW = 31.25$ kHz, radically differ from the results of experiments with $SF = 7$ and 10, performed at the same BW. In experiment No. 15, during which NORBY transmitted approximately 60 data packets of size $L = 143$ bytes, none were received at the ground station. The results of experiment No. 14, performed with the same LoRa parameters but $L = 55$ bytes, are shown in Fig. 13. It can be seen that out of 118 packets sent from the satellite, the ground station received only four in the time interval from approximately $-$ -115 s to -90 s.

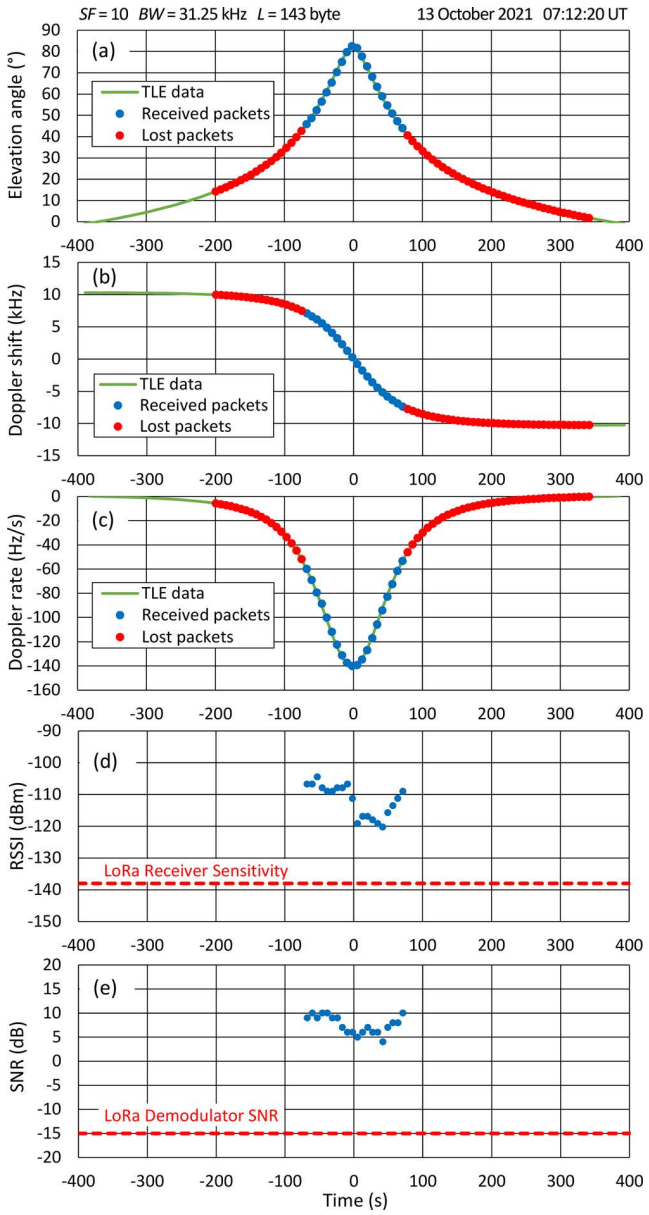

FIGURE 11. Same as Fig. 7 but for experiment No. 11 with the LoRa modulation parameters $SF = 10$, $BW = 31.25$ kHz and $L = 143$ bytes

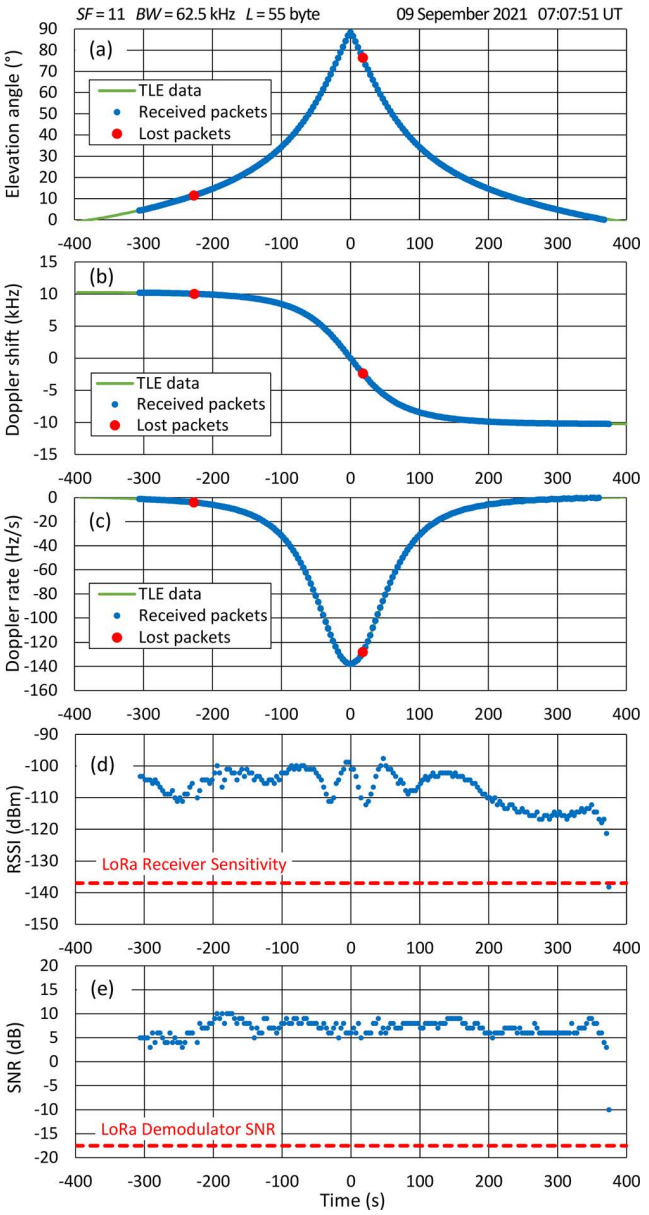

FIGURE 12. Same as Fig. 7 but for experiment No. 12 with the LoRa modulation parameters $SF = 11$, $BW = 62.5$ kHz and $L = 55$ bytes.

The ground station began to receive packets when the Doppler shift ΔF_D and the total frequency offset ΔF decreased to 8.8 kHz and 7.9 kHz, respectively. Then, the reception of data packets from the satellite stopped at Doppler shift $\Delta F_D = 8.0$ kHz and Doppler rate $\Delta F'_D = -41$ Hz/s. The total frequency shift ΔF and the rate of its change $\Delta F'$ at this moment were equal to 7.2 kHz and -41 Hz/s, respectively.

A decrease in ΔF_D to zero at $t = 0$ s indicates that the Doppler shift (static Doppler effect) cannot cause packet loss in this case. The signal level and signal-to-noise ratio at the input of the ground station LoRa receiver were much larger than the LoRa receiver sensitivity and LoRa demodulator SNR during the successfully received packets (see Figures 13d and 13e). Therefore, the only explanation for the loss of data packets after the -90th second is the destruction of the LoRa satellite-to-ground radio channel, caused by a large absolute value of $\Delta F'_D$, that is, the dynamic Doppler effect.

D. SF = 12

Five experiments were performed with $SF = 12$ (Table 2). In experiment No. 20, at $BW = 31.25$ kHz and $L = 55$ bytes, the ground station did not receive a single packet out of about 70 transmitted from the satellite. This result is similar to that obtained in the experiment described above with $SF = 11$ and $BW = 31.25$ kHz. The lack of LoRa radio communication with the satellite in this case appears to be due to both static and dynamic Doppler effects. However, the complete absence of any data in the experiment did not allow us to draw any

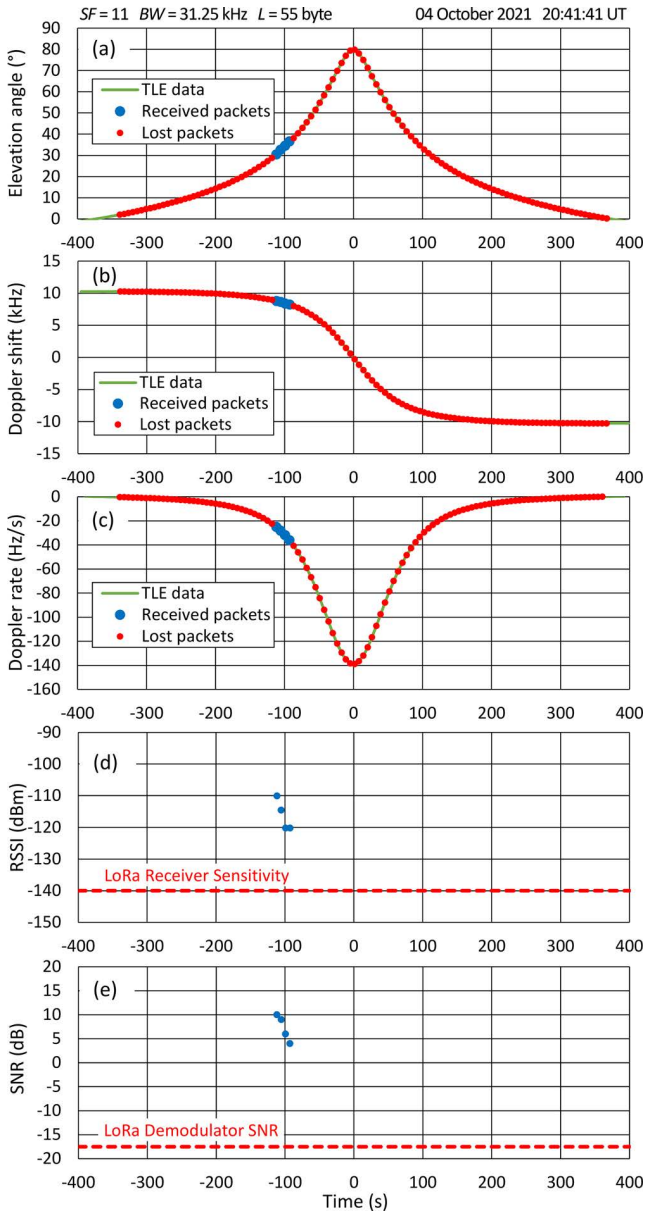

FIGURE 13. Same as Fig. 7 but for experiment No. 14 with the LoRa modulation parameters $SF = 11$, $BW = 31.25$ kHz and $L = 55$ bytes.

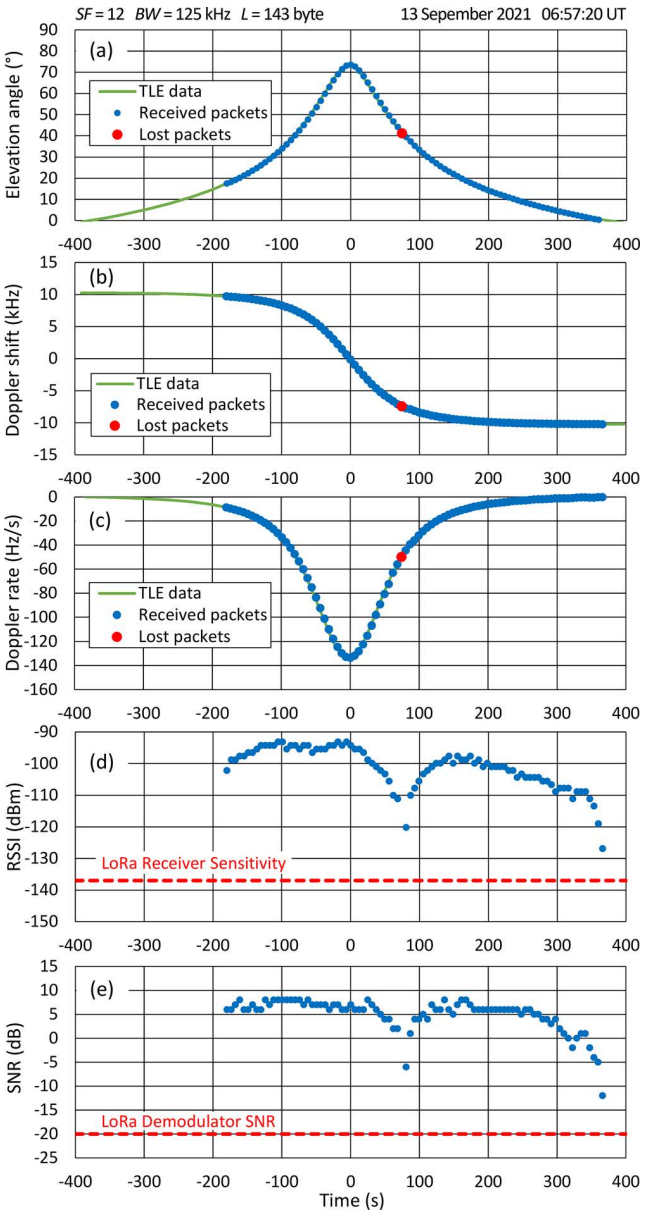

FIGURE 14. Same as Fig. 7 but for experiment No. 17 with the LoRa modulation parameters $SF = 12$, $BW = 125$ kHz and $L = 143$ bytes.

quantitative conclusions about the influence of the Doppler effect on the LoRa satellite-to-ground radio channel.

The other four experiments with $SF = 12$ were carried out with a wider spread spectrum modulation bandwidth of 125 kHz and 62.5 kHz. Experiments No. 16 and No. 17 were carried out with the spreading factor $SF = 125$ kHz and packet lengths $L = 55$ and 143 bytes, respectively. In the first experiment, a single packet was lost at a satellite elevation angle of about 1° when the satellite was approaching the horizon and the signal to noise ratio at the receiver input decreased to approximately −20 dB, that is, to LoRa demodulator SNR. In the second experiment, packet loss occurred owing to a short-term unsuccessful orientation of the satellite during its rotation, which caused a decrease in the signal level at the receiver input (see Fig. 14). No impact of the Doppler effect on the LoRa satellite-to-ground radio channel was observed in these experiments.

The results of experiments No. 18 and No. 19 with $SF = 12$ and $BW = 62.5$ kHz are shown in Fig. 15 and Fig. 16 for $L = 55$ and 143 bytes, respectively. It can be seen that with these LoRa modulation parameters, there was no radio communication with NORBY at high satellite elevation angles, that is, in the region of maximum absolute values of the Doppler rate. In experiment No. 18, data packets transmitted from NORBY ceased to be received by the ground station at $t = -89$ s, when the Doppler rate $\Delta F'_D$ increased in absolute value to 38 Hz/s (see Fig. 15c). The reception of data packets resumed at $t = 93$ s when the absolute value

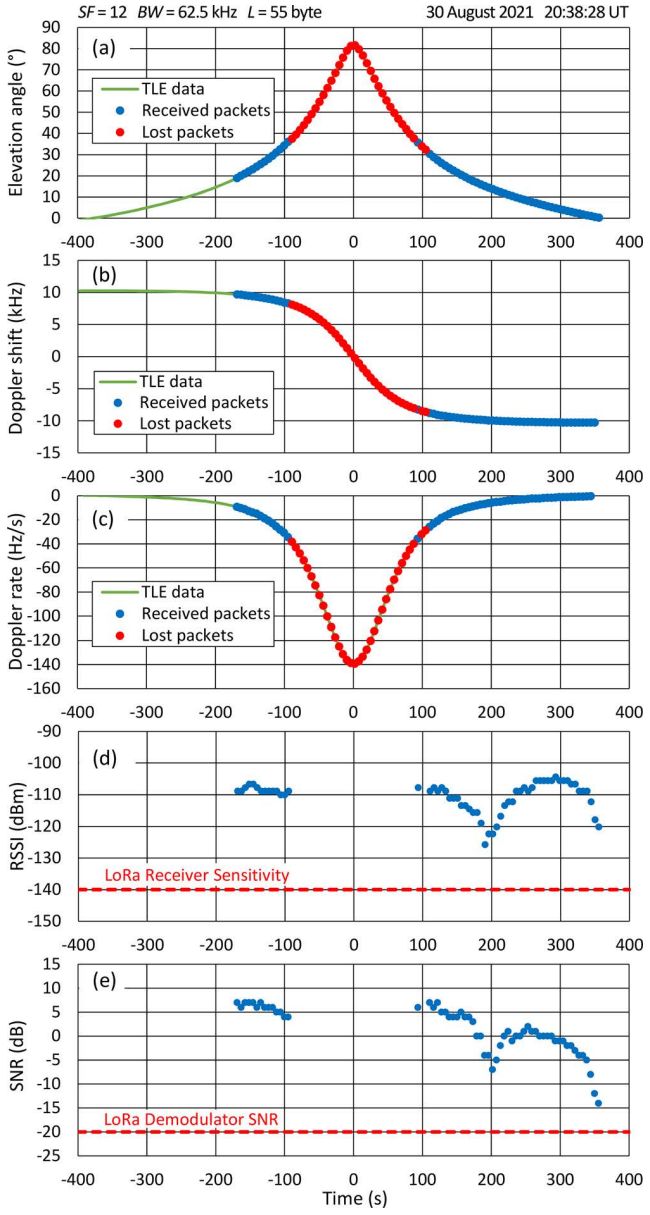

FIGURE 15. Same as Fig. 7 but for experiment No. 18 with the LoRa modulation parameters $SF = 12$, $BW = 62.5$ kHz and $L = 55$ bytes.

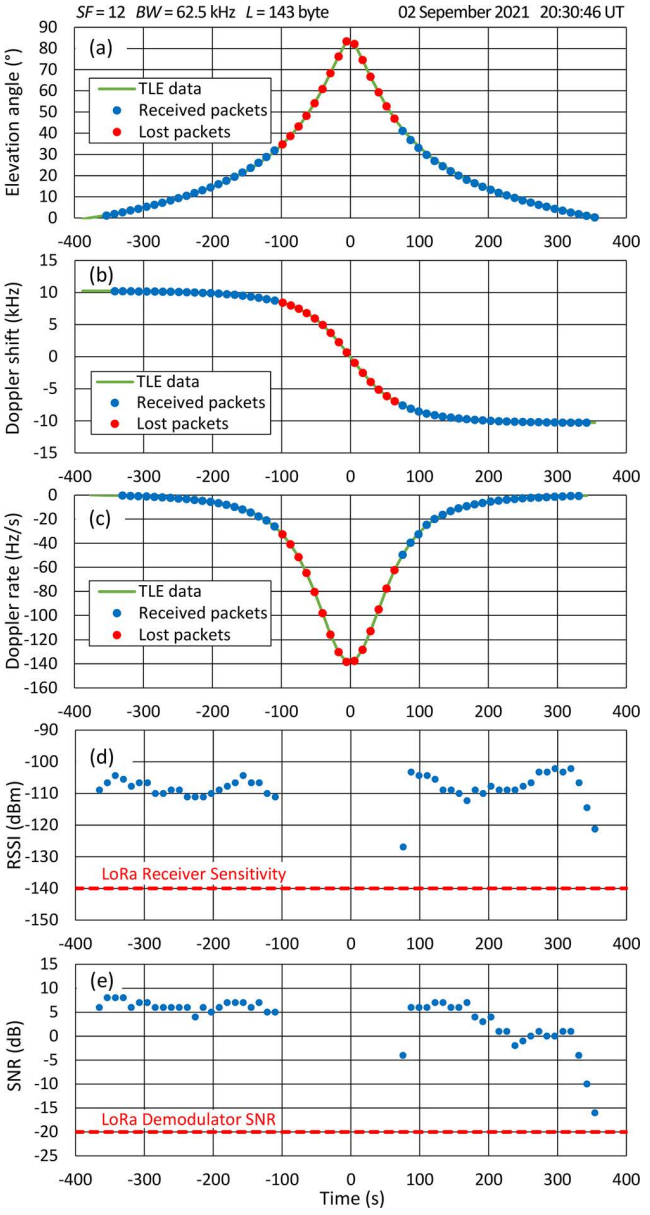

FIGURE 16. Same as Fig. 7 but for experiment No. 19 with the LoRa modulation parameters $SF = 12$, $BW = 62.5$ kHz and $L = 143$ bytes.

of $\Delta F'_D$ decreased to 36 Hz/s as the satellite moved away from the ground station. According to the FER data, the absolute values of $\Delta F'$ at these times were 42 and 32 kHz/s, respectively. Subsequently, two packets were lost at the 99$^{\text{th}}$ and 105$^{\text{th}}$ s, and the LoRa radio link was finally restored at $t = 110$ s. We could not clearly determine the reason for the loss of these two packets.

Similarly, in experiment No. 19, data packets began to be lost at $t = -98$ s and $\Delta F'_D = -33$ Hz/s, and received again at $t = 75$ s and $\Delta F'_D = -44$ Hz/s (see Fig. 16c). $\Delta F'$ at these times were equal to -29 kHz/s and -43 kHz/s, respectively.

We see the only reason that can explain the destruction of the LoRa satellite-to-ground radio channel observed in experiments No. 18 and No. 19 at high satellite elevation angles. This is a rapid change in the Doppler frequency shift, that is, the dynamic Doppler effect. Thus, in these experiments, the effect of the disruption of LoRa radio communication during the passage of a satellite directly over a ground station, predicted in [13] based on laboratory studies, was observed for the first time.

IV. SUMMARIZING AND CONCLUSION

We have presented here the results of the first flight tests of LoRa modulation in a satellite-to-ground radio channel. The tests were carried out using the NORBY CubeSat, which is located in a low-Earth orbit with an altitude of approximately 560 km. The main purpose of the flight tests was to verify in real space conditions the robustness of the LoRa modulation

TABLE 3. General results of LoRa modulation testing in the NORBY flight experiments.

Exp. No.	*SF*	*BW*, kHz	*L*, byte	Number of packets			Causes of the losses
				Sent	Received	Lost	
1	7	500	143	773	748	25	Weak signal due to CubeSat orientation (12) Low SNR due to ambient noise (12) Unclear (1)
2	7	125	55	597	518	79	Weak signal due to CubeSat orientation
3	7	125	143	381	380	1	Unclear
4	7	62.5	55	431	431	0	–
5	7	62.5	143	493	492	1	Low SNR due to ambient noise
6[a]	7	31.25	55	554	120	434	Doppler shift
7[a]	7	31.25	143	348	78	270	Doppler shift
8	10	62.5	55	216	216	0	–
9	10	62.5	143	230	227	3	Low SNR due to ambient noise
10[a]	10	31.25	55	184	42	142	Doppler shift
11[a]	10	31.25	143	75	20	55	Doppler shift
12	11	62.5	55	190	188	2	Unclear
13	11	62.5	143	95	95	0	–
14[a]	11	31.25	55	118	4	114	Doppler shift and Doppler rate
15[a]	11	31.25	143	~60	0	~60	Doppler shift and Doppler rate
16	12	125	55	213	212	1	Weak signal near the horizon
17	12	125	143	89	88	1	Weak signal due to CubeSat orientation
18[a]	12	62.5	55	93	59	34	Doppler rate (32), Unclear (2)
19[a]	12	62.5	143	63	48	15	Doppler rate
20[a]	12	31.25	55	~70	0	~70	Doppler shift and Doppler rate

[a]Shaded are experiments in which the Doppler shift and/or Doppler rate caused disruption of the radio link.

against the Doppler effect, determined in laboratory studies [13]. It was also supposed to check the maximum allowable frequency offset between the transmitter and receiver given in the datasheet of the LoRa SX1278 transmitter [14]. An important task was to detect the effect of radio communication disruption owing to the dynamic Doppler effect when the satellite passed directly over the ground station, which was predicted in [13].

Testing was performed with spreading factor *SF* from 7 to 12 and spread spectrum modulation bandwidth *BW* from 31.25 kHz to 500 kHz. Data packets with sizes $L = 55$ bytes and 143 bytes were used in the experiments.

The general results of the LoRa modulation testing obtained during the flight experiments are listed in Table 3. For the 20 radio sessions with the NORBY CubeSat, during which the experiments were carried out, 5273 data packets were transmitted from the satellite. The ground station successfully received only 3966 of them. The remaining 1307 packets were lost. A total of 109 packets were lost owing

TABLE 4. Results of NORBY experiments in which LoRa radio communication was disrupted due to the Doppler effect.

SF	*BW*, kHz	*L*, byte	Static Doppler effect ΔF_{max}		Dynamic Doppler effect $\Delta F'_{max}$	
			kHz	% of *BW*	Hz/s	ppm/s
7	31.25	55	7.8	24.9		
7	31.25	143	7.7	24.5		
10	31.25	55	7.8	24.9		
10	31.25	143	7.7	24.6		
11	31.25	55	7.9	25.1	41	0.09
12	62.5	55			37	0.09
12	62.5	143			36	0.08
12[a]	125				>143	>0.33

[a]The dynamic Doppler effect is predicted to affect LoRa radio communication in orbits below 550 km [13].

to weak signal or low signal-to-noise ratio at the input of the LoRa receiver, six packets were lost for an unknown reason, and 1192 packets were not received by the ground station owing to the Doppler effect. The destructive impact of the Doppler effect on the satellite-to-ground LoRa radio channel was recorded in nine communication sessions (shaded rows in Table 3).

The static Doppler effect was clearly manifested in four experiments with $SF = 7$ and $SF = 10$ at spread spectrum modulation bandwidth $BW = 31.25$ kHz (Nos. 6, 7, 10, and 11 in Table 3). The maximum frequency offset ΔF_{max} between the carrier frequencies of the LoRa receiver and the received signal, above which the LoRa radio link was disrupted, was determined in each experiment. In total, in four experiments, we obtained eight values of ΔF_{max}, four of which were obtained when the satellite approached the ground station and the rest when moving away. The averages of the two ΔF_{max} values obtained from each experiment are listed in Table 4. The ΔF_{max} value averaged over all data is 7.73 Hz or 24.7% of *BW*. The ΔF_{max} values obtained in the experiments are in very good agreement with the maximum tolerated frequency offset between the transmitter and receiver of $0.25 \times BW$, specified in the datasheet of the LoRa SX1278 transceiver [14].

In experiments conducted for the first time under natural conditions, it was possible to detect the destructive effect of the dynamic Doppler effect on the LoRa radio channel. It manifested itself most clearly in experiments No. 18 and No. 19, which were performed at $SF = 12$ and $BW = 62.5$ kHz. With this *BW*, the LoRa modulation has very high immunity to static Doppler at all the tested *SF* values. Outside (but close to) the outage zone, the signal level and signal-to-noise ratio at the input of the ground station LoRa receiver were much larger than the LoRa receiver sensitivity and LoRa demodulator SNR. Therefore, the observed disruption of radio communication with the satellite in the region of maximum absolute values of the Doppler rate (see Figures 15 and 16) can naturally be explained by the influence of the dynamic Doppler effect. In these experiments, four values of the rate of change of the total frequency

TABLE 5. Doppler effect restrictions on the use of LoRa modulation in radio communications with LEO satellites.

BW, kHz	*SF*			
	7	10	11	12
125	No restrictions	No restrictions	No restrictions	Dynamic Doppler effect (below 550 km)
62.5	No restrictions	No restrictions	No restrictions	Dynamic Doppler effect
31.25	Static Doppler effect	Static Doppler effect	Static and Dynamic Doppler effect	Static and Dynamic Doppler effect

offset $\Delta F'_{\max}$ were obtained, above which a disruption of the LoRa radio communication was observed. The averages of the two $\Delta F'_{\max}$ values obtained from each experiment are listed in Table 4. The average value of $\Delta F'_{\max}$ is 36.6 Hz/s or 0.08 ppm/s.

In laboratory experiments [13], a value of $\Delta F'_{\max} = 0.33$ ppm/s (144 Hz/s for the NORBY radio frequency) was obtained also for $SF = 12$ but at $BW = 125$ kHz. Unfortunately, it was not possible to verify this result in the NORBY experiments because the maximum Doppler rate in the NORBY orbit is only 143 Hz/s in absolute value. Higher Doppler rates exist only in the lower orbits below approximately 550 km. However, the effect of the disruption of LoRa radio communication when the satellite passes directly over the ground station, predicted in [13], was clearly detected in the NORBY experiments with BW = 62.5 kHz.

The LoRa modulation at $SF = 12$ and $BW = 31.25$ kHz proved to be unsuitable for use in radio communication with LEO satellites. In experiment No. 20, with these LoRa modulation parameters, the ground station did not receive any of the data packets transmitted by NORBY. At low elevation angles of the satellite, the LoRa radio communication did not work because of the static Doppler effect, and at high elevation angles, due to the dynamic Doppler effect.

For $SF = 11$ and $BW = 31.25$ kHz, the LoRa modulation behaves similarly. However, in experiment No. 14, radio communication with the satellite worked for a short time interval of approximately 25 s when NORBY approached the ground station. Apparently, in this time interval, the Doppler shift has already decreased to an acceptable level for the operation of LoRa radio communication, and the Doppler rate has not yet increased enough to disrupt radio communication. This enabled the determination of $\Delta F_{\max} = 7.9$ kHz and $\Delta F'_{\max} = 41$ Hz/s for these *SF* and *BW*.

The values of $\Delta F_{\max}$ and $\Delta F'_{\max}$ obtained from the NORBY experiments are summarized in Table 4. For comparison, Table 4 also shows the values of $\Delta F'_{\max}$ for $SF = 12$ and $BW = 125$ kHz obtained in laboratory studies of LoRa modulation [13]. Table 4 shows that all the $\Delta F_{\max}$ values obtained in the NORBY experiments are in very good agreement with the maximum tolerated frequency offset between the transmitter and receiver, as given in the datasheet of the LoRa transceiver SX1278 ($\Delta F_{\max} = 0.25 \times BW$) [14]. However, the datasheet [14] does not contain any information regarding the criteria for LoRa modulation stability when changing the frequency offset. The results of laboratory experiments [13] concerning $\Delta F'_{\max}$ for $SF = 12$ and $BW = 125$ kHz proved impossible to verify in the NORBY orbit. There are no other experimental data on the stability of the LoRa modulation to $\Delta F'$; therefore, there is nothing to compare the obtained values of $\Delta F'_{\max}$ with.

Table 5 shows in a visual form the Doppler effect restrictions on the use of LoRa modulation in radio communications with LEO satellites obtained in the NORBY experiments. For $SF \leq 11$ and $BW \geq 62.5$ kHz, there are no restrictions on the use of LoRa modulation in satellite radio communications. For $BW = 31.25$ kHz, the LoRa radio channel is affected by the static Doppler effect. Radio communication with the satellite is possible in this case only at high elevation angles of the satellite when flying directly over the ground station. For $SF = 12$, on the contrary, the dynamic Doppler effect becomes significant and radio communication is possible only at small satellite elevation angles at large distances from the ground station. In both latter cases, the duration of the communication session is significantly reduced due to the Doppler effect.

In the case of $SF = 11$ and 12 at $BW = 31.25$ kHz, both static and dynamic Doppler effects catastrophically affected the LoRa radio channel. In this case, LoRa radio communication with a satellite in a low-Earth orbit is not possible.

The restrictions imposed by the Doppler effect on the use of LoRa modulation relate primarily to LoRa modes that provide maximum receiver sensitivity and, consequently, the maximum radio communication range with minimum transmitter power. Therefore, they are extremely important for the satellite Internet of Things. Our results show that the most super-sensitive LoRa modulation modes with $SF = 11$ and 12 at $BW \leq 31.25$ kHz are unsuitable for use in LEO satellite IoT networks due to the Doppler effect. This is the case unless some system is used to correct the carrier frequency of the LoRa receiver or transmitter on the base of the predicted Doppler shift and Doppler rate.

The use of LoRa modulation modes with intermediate sensitivity, at which the influence of the Doppler effect begins, reduces the coverage area of the radio communication by one satellite. The static Doppler effect reduces the coverage area near the horizon. The dynamic Doppler effect results in a "hole" in the center of the coverage area directly below the satellite. The use of these LoRa modes in IoT satellite networks complicates the task of creating a globally contiguous coverage area using the LEO satellite constellation.

LoRa modulation modes with $SF \leq 11$ and BW $>$ 31.25 kHz can be used in satellite IoT without any limitations caused by the Doppler effect. The Doppler limits on the use of LoRa modulation in satellite radio communications obtained in the NORBY experiments are applicable to satellites in any orbit. However, it should be borne in mind that the orbital velocity of a satellite decreases with increasing orbit altitude.

As a result, Doppler-induced restrictions become less critical when the IoT satellite constellation is placed in a higher orbit.

In general, the satellite experiments conducted made it possible to determine the limits of applicability of LoRa modulation in radio communications with LEO satellites. In particular, for the first time, the disruption of radio communication due to the dynamic Doppler effect was detected when the satellite passed directly over the ground station.

In conclusion, we would like to note that we are planning to test our results for the 868 MHz and 2.4 GHz bands in the near future on the new NORBY-2 CubeSat.

APPENDIX

GLOSSARY OF ACRONYMS

ADCS	Attitude Determination and Control System.
BRC	On-Board Radio Complex.
BW	Band Width.
CSS	Chirp Spread Spectrum.
EPS	Electrical Power System.
FER	Frequency Error Indication.
FSK	Frequency Shift Keying.
GLONASS	Global Navigation Satellite System.
GFSK	Gaussian Frequency Shift Keying.
GMSK	Gaussian Minimum Shift Keying.
IoT	Internet of Things.
LEO	Low Earth Orbit.
LoRa	Long Range.
MSK	Minimum-Shift Keying.
PCB	Printed Circuit Board.
RF	Radio Frequency.
RSSI	Received Signal Strength Indicator.
SATCAT	Satellite Catalog.
SF	Spreading Factor.
SNR	Signal to Noise Ratio.
TLE	Two-Line Element

REFERENCES

[1] C. A. Hornbuckle, "Fractional-N synthesized chirp generator," U.S. Patent 7 791 415 B2, Sep. 7, 2010.

[2] C. Goursaud and J. M. Gorce, "Dedicated networks for IoT: PHY/MAC state of the art and challenges," *EAI Endorsed Trans. Internet Things*, vol. 1, no. 1, Oct. 2015, Art. no. 150597.

[3] A. Augustin, J. Yi, T. Clausen, and W. Townsley, "A study of LoRa: Long range & low power networks for the Internet of Things," *Sensors*, vol. 16, no. 9, p. 1466, Sep. 2016.

[4] *LoRa™ Modulation Basics, Application Note AN1200.22, Rev. 2*, Semtech Corp., Camarillo, CA, USA, May 2015. [Online]. Available: https://semtech.my.salesforce.com/sfc/p/#E0000000JelG/a/2R0000001OJa/2BF2MTeiqIwkmxkcjjDZzalPUGlJ76lLdqiv.30prH8

[5] L. Vangelista, "Frequency shift chirp modulation: The LoRa modulation," *IEEE Signal Process. Lett.*, vol. 24, no. 12, pp. 1818–1821, Dec. 2017.

[6] Z. Qu, G. Zhang, H. Cao, and J. Xie, "Leo satellite constellation for Internet of Things," *IEEE Access*, vol. 5, pp. 18391–18401, 2017.

[7] Y. Qian, L. Ma, and X. Liang, "Symmetry chirp spread spectrum modulation used in LEO satellite Internet of Things," *IEEE Commun. Lett.*, vol. 22, no. 11, pp. 2230–2233, Nov. 2018.

[8] J. A. Fraire, S. Henn, F. Dovis, R. Garello, and G. Taricco, "Sparse satellite constellation design for LoRa-based direct-to-satellite Internet of Things," in *Proc. IEEE Global Commun. Conf.*, Dec. 2020, Art. no. 9348042.

[9] M. Centenaro, C. E. Costa, F. Granelli, C. Sacchi, and L. Vangelista, "A survey on technologies, standards and open challenges in satellite IoT," *IEEE Commun. Surveys Tuts.*, vol. 23, no. 3, pp. 1693–1720, 3rd Quart., 2021.

[10] I. F. Akyildiz and A. Kak, "The Internet of Space Things/CubeSats: A ubiquitous cyber-physical system for the connected world," *Comput. Netw.*, vol. 150, pp. 134–149, Feb. 2019.

[11] J. Kua, S. W. Loke, C. Arora, N. Fernando, and C. Ranaweera, "Internet of Things in space: A review of opportunities and challenges from satellite-aided computing to digitally-enhanced space living," *Sensors*, vol. 21, no. 23, p. 8117, Dec. 2021.

[12] A. Doroshkin, A. Zadorozhny, O. Kus, V. Prokopyev, and Y. Prokopyev, "Laboratory testing of LoRa modulation for CubeSat radio communications," in *Proc. MATEC Web Conf.*, vol. 158, Mar. 2018, p. 01008.

[13] A. A. Doroshkin, A. M. Zadorozhny, O. N. Kus, V. Y. Prokopyev, and Y. M. Prokopyev, "Experimental study of LoRa modulation immunity to Doppler effect in CubeSat radio communications," *IEEE Access*, vol. 7, pp. 75721–75731, 2019.

[14] *SX1276/77/78/79—137 MHz to 1020 MHz Low Power Long Range Transceiver, Datasheet, Rev. 7*, Semtech Corp., Camarillo, CA, USA, May 2020. [Online]. Available: https://semtech.my.salesforce.com/sfc/p/#E0000000JelG/a/2R0000001Rc1/QnUuV9TviODKUgt_rpBlPz.EZA_PNK7Rpi8HA5.Sbo

[15] G. Colavolpe, T. Foggi, M. Ricciulli, Y. Zanettini, and J.-P. Mediano-Alameda, "Reception of LoRa signals from LEO satellites," *IEEE Trans. Aerosp. Electron. Syst.*, vol. 55, no. 6, pp. 3587–3602, Dec. 2019, doi: 10.1109/TAES.2019.2909336.

[16] C. A. Hofmann, K.-U. Storek, and A. Knopp, "Impact of phase noise and oscillator stability on ultra-narrow-band-IoT waveforms for satellite," in *Proc. IEEE Int. Conf. Commun.*, Jun. 2021, pp. 1–6.

[17] *SX1261/2 Long Range, Low Power, Sub-GHz RF Transceiver, Data Sheet, Rev. 2.1*, Semtech Corp., Camarillo, CA, USA, Dec. 2021. [Online]. Available: https://semtech.my.salesforce.com/sfc/p/#E0000000JelG/a/2R000000Un70/ZHJLT5MqbYVJJZCeCYgXjCek0iAq88aBOmZOU6Vgskk

[18] L. Fernandez, J. A. Ruiz-De-Azua, A. Calveras, and A. Camps, "Assessing LoRa for satellite-to-earth communications considering the impact of ionospheric scintillation," *IEEE Access*, vol. 8, pp. 165570–165582, 2020.

[19] C. A. Hofmann and A. Knopp, "Ultranarrowband waveform for IoT direct random multiple access to GEO satellites," *IEEE Internet Things J.*, vol. 6, no. 6, pp. 10134–10149, Dec. 2019.

[20] R. Ortigueira, J. A. Fraire, A. Becerra, T. Ferrer, and S. Cespedes, "RESS-IoT: A scalable energy-efficient MAC protocol for direct-to-satellite IoT," *IEEE Access*, vol. 9, pp. 164440–164453, 2021.

[21] M. A. Ullah, K. Mikhaylov, and H. Alves, "Enabling mMTC in remote areas: LoRaWAN and LEO satellite integration for offshore wind farm monitoring," *IEEE Trans. Ind. Informat.*, vol. 18, no. 6, pp. 3744–3753, Jun. 2022.

[22] Q. Verspieren, T. Matsumoto, Y. Aoyanagi, T. Fukuyo, T. Obata, S. Nakasuka, G. Kwizera, and J. Abakunda, "Store-and-forward 3U CubeSat project TRICOM and its utilization for development and education: The cases of TRICOM-1R and JPRWASAT," *Trans. Jpn. Soc. Aeronaut. Space Sci.*, vol. 63, no. 5, pp. 206–211, 2020.

[23] V. Y. Prokopyev *et al.*, "NORBY CubeSat nanosatellite: Design challenges and the first flight data," *J. Phys., Conf. Ser.*, vol. 1867, no. 1, Apr. 2021, Art. no. 012038.

[24] (Jan. 11, 2022). *Lacuna and Semtech Expand LoRaWAN® Coverage Through IoT to Satellite Connectivity*. [Online]. Available: https://lacuna.space/lacuna-and-semtech-expand-lorawan-coverage-through-iot-to-satellite-connectivity/

[25] A. Pelemeshko, A. Kolesnikova, A. Melkov, V. Prokopyev, and A. Zadorozhny, "High-precision CubeSat sun sensor coupled with infrared earth horizon detector," *IOP Conf. Ser., Mater. Sci. Eng.*, vol. 734, no. 1, Jan. 2020, Art. no. 012012.

[26] RF HAMDESIGN B.V. Microwave Equipment & RF Parts. *SPID, Type BIG-RAS/HR Azimuth & Elevation Rotor*. Drachten, The Netherlands. Accessed: May 20, 2022. [Online]. Available: https://www.rfhamdesign.com/downloads/spid-bigras_hr-specifications.pdf

[27] *Gpredict*. Accessed: May 20, 2022. [Online]. Available: http://gpredict.oz9aec.net

[28] *Satellite Catalog (SATCAT)*. Accessed: May 20, 2022. [Online]. Available: https://celestrak.com/satcat/search.php

[29] G. R. Dunlop, P. J. Ellis, and N. V. Afzulpurkar, "The satellite tracking keyhole problem: A parallel mechanism mount solution," *Trans. Inst. Prof. Eng. New Zealand, Elect./Mech./Chem. Eng. Sect.*, vol. 20, no. 1, pp. 1–7, Nov. 1993.

ALEXANDER M. ZADOROZHNY graduated in radio physics from the Department of Physics, Novosibirsk State University, Russia, in 1971, and received the Ph.D. degree in atmospheric physics from Novosibirsk State University, in 1982.

He is currently a Leading Research Fellow with the Division for Aerospace Research, Novosibirsk State University, where he is also an Associate Professor with the Department of General Physics. His research interests include the composition and electrodynamics of the middle atmosphere, Earth's ozone layer, noctilucent clouds, external influences on the middle atmosphere, and rocket and satellite experiments.

Dr. Zadorozhny is a member of the American Geophysical Union and an Associate of the Committee on Space Research.

ALEXANDER A. DOROSHKIN graduated in radio physics from the Department of Physics, Novosibirsk State University, Russia, in 1990.

He is currently an Assistant Professor with the Department of General Physics, Novosibirsk State University, where he is also a Lead Engineer with the Division for Aerospace Research. His research interests include electronics engineering, wireless communication, and communications for the satellite-based Internet of Things, industrial automation, and rocket and satellite experiments.

VASILY N. GOREV graduated in fluid mechanics from the Department of Physics, Novosibirsk State University, Russia, in 2004, and received the Ph.D. degree in fluid and plasma mechanics from Novosibirsk State University, in 2007.

He is currently a Senior Research Fellow with the Division for Aerospace Research, Novosibirsk State University, where he is also an Associate Professor with the Department of General Physics. His research interests include the spacecraft ballistic, thermal, and mechanical engineering of spacecraft subsystems and small satellites.

ALEXANDER V. MELKOV graduated in management in engineering systems from the Faculty of Automation and Computer Engineering, Novosibirsk State Technical University, Russia, in 2011.

He is currently a Lead Engineer at OKB Fifth Generation Ltd., Novosibirsk, Russia. His research interests include electronics engineering, wireless communication, embedded programming, and small satellite design.

ANTON A. MITROKHIN graduated in physical and technical informatics from the Department of Physics, Novosibirsk State University, Russia, in 2020, where he is currently pursuing the Ph.D. degree.

He is currently a Software Engineer with OKB Fifth Generation Ltd., Novosibirsk, Russia. His research interests include the development of a network of ground stations to increase the connection time for satellites on LEO, wireless communication, and satellite-based Internet of Things.

VITALIY YU. PROKOPYEV graduated in quantum electronics from the Department of Physics, Novosibirsk State University, Russia, in 2004.

He is currently the Head of the Division for Aerospace Research, Novosibirsk State University, where he is also an Assistant Professor with the Department of General Physics. His research interests include electronics engineering in space instrumentation, embedded programming, and small satellite design.

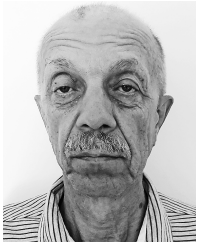

YURI M. PROKOPYEV graduated in radio physics from the Department of Physics, Novosibirsk State University, Russia, in 1981, and received the Ph.D. degree in technical sciences from Novosibirsk State University, in 1995.

He is currently the Head of the Laboratory of Space Experiments, Novosibirsk State University, where he is also an Associate Professor with the Department of General Physics. His research interests include space instrumentation, space experiments, and the influence of space factors on spacecraft.